

6.3.1 Basinwide distribution

The map of upland-erosion potential (Figure 6-7) provides insights into differences in upland-erosion potential across the Lake Tahoe Basin. Some of these, such as the generally green areas (lowest classes) in the eastern quadrant were to be expected as this represents the dry side of the lake where suspended-sediment yields are low. Similar areas, such as in the southwest part of the basin are consistent with the generally low suspended-sediment yields emanating from these watersheds (and documented in Chapter 3. Areas of high upland-erosion potential are concentrated in the northwest parts of the basin, particularly in headwaters areas of Burton, Ward and Blackwood Creeks, as well as in the Homewood and Madden Creek watersheds. Sizeable high erosion-potential areas are also depicted in Third Creek and several other northern quadrant streams.

6.3.2 Determination of Areas Covered By Erosion Classes

Conversion of erosion-class data to areas simplified subsequent analysis between upland-erosion potential and suspended-sediment transport rates calculated from measured flow and sediment-concentration data. Areas occupied by each erosion-potential class were determined within individual watersheds and above gaging stations. Initially, the raster was converted to a vector layer using the convert raster to feature function. This conversion created polygons representing erodibility classes for the entire basin. Secondly, this new vector layer was intersected with the watershed outline layer creating a new set of polygons representing erodibility classes separated by watershed. The areas of each erosion class within a given watershed were added to determine whether the total area calculated by the ArcView zonal-statistics analysis corresponded to the actual area of the watershed. Table 6-8 lists the 63 watersheds draining Lake Tahoe in decreasing order of the percentage of their basin area covered by high erosion classes 4 and 5 (orange and red areas; Figure 6-7).

Table 6-8. Percentage of the area of each watershed draining to Lake Tahoe covered by the two highest upland-erosion potential classes (percentage of red plus orange areas in Figure 6-7).

Watershed	Percent class 4	Percent class 5	Percent of two highest classes
HOMEWOOD CREEK	68.3	4.34	72.7
KINGS BEACH	67.7	0.00	67.7
DOLLAR CREEK	65.5	0.57	66.1
GRIFF CREEK	57.2	0.07	57.2
BARTON CREEK	44.8	5.98	50.7
EAGLE ROCK	47.3	0.00	47.3
BURTON CREEK	43.5	3.29	46.8
MADDEN CREEK	43.4	2.79	46.2
WARD CREEK	40.1	2.82	43.0
LAKE FOREST CREEK	42.0	0.00	42.0

EAST STATELINE POINT	38.0	0.00	38.0
WATSON	37.5	0.38	37.9
TAHOE VISTA	37.4	0.07	37.5
SECOND CREEK	26.7	0.52	27.2
BLACKWOOD CREEK	26.3	0.92	27.2
QUAIL LAKE CREEK	26.0	0.93	26.9
BURNT CEDAR CREEK	25.7	0.45	26.2
FIRST CREEK	23.0	0.00	23.0
CEDAR FLATS	22.5	0.00	22.5
INCLINE CREEK	18.7	0.91	19.7
CAMP RICHARDSON	11.6	0.00	11.6
BIJOU CREEK	8.4	0.00	8.4
CARNELIAN CANYON	7.9	0.00	7.9
UPPER TRUCKEE RIVER	7.9	0.00019	7.9
MKINNEY CREEK	6.7	0.08	6.8
CAVE ROCK	6.1	0.39	6.5
WOOD CREEK	5.1	0.03	5.1
CARNELIAN BAY CREEK	4.6	0.00	4.6
TALLAC CREEK	4.6	0.00	4.6
GENERAL CREEK	3.7	0.00	3.7
BLISS STATE PARK	3.6	0.04	3.6
THIRD CREEK	3.6	0.00	3.6
EAGLE CREEK	3.4	0.02	3.4
LINCOLN CREEK	3.3	0.00	3.3
BIJOU PARK	2.8	0.00	2.8
GLENBROOK CREEK	2.5	0.00	2.5
TAHOE STATE PARK	2.5	0.00	2.5
SIERRA CREEK	2.3	0.00	2.3
PARADISE FLAT	2.1	0.00	2.1
SECRET HARBOR CREEK	2.0	0.00	2.0
CASCADE CREEK	1.5	0.00	1.5
RUBICON CREEK	1.4	0.00	1.4
EDGEWOOD CREEK	1.2	0.00	1.2
TAYLOR CREEK	1.1	0.00098	1.1
MEEKS	1.1	0.00	1.1
TROUT CREEK	0.7	0.00	0.7
SLAUGHTER HOUSE	0.3	0.00	0.3
MARLETTE CREEK	0.2	0.00	0.2
LONELY GULCH CREEK	0.1	0.00	0.1
BURKE CREEK	0.1	0.00	0.1
NORTH LOGAN HOUSE CREEK	0.1	0.00	0.1

MILL CREEK	0.0	0.00	0.0
BLISS CREEK	0.0	0.00	0.0
BONPLAND	0.0	0.00	0.0
DEADMAN POINT	0.0	0.00	0.0
LOGAN HOUSE CREEK	0.0	0.00	0.0
MCFAUL CREEK	0.0	0.00	0.0
NORTH ZEPHYR CREEK	0.0	0.00	0.0
SAND HARBOR	0.0	0.00	0.0
SKYLAND	0.0	0.00	0.0
TRUCKEE RIVER	0.0	0.00	0.0
TUNNEL CREEK	0.0	0.00	0.0
ZEPHYR CREEK	0.0	0.00	0.0

6.3.3 Results

Interpretation of data describing the upland-erosion potential index centers on comparing suspended-sediment transport data calculated at gaging stations with the percentage of high-erosion potential classes (percentage of red areas plus orange areas in Figure 6-7) in each basin or upstream of each gaging station. Similar regression characteristics were obtained when working with several variables representing annual suspended-sediment transport rates such as load (T/y), yield (T/km²), and concentration (g/m³) for both index stations and for areas above all gaging stations. In all cases, three stations plotted anomalously above the fitted regression: Blackwood Creek, Ward Creek and Third Creek, all having substantial contributions from channel sources. The most encouraging results were obtained using suspended-sediment transport data from all stations with median, annual data expressed as annual yields (Figure 6-8); $r^2 = 0.63$. It seems from the data in Figure 6-8 that there may be a threshold value or range of values above which the processes represented by the upland-erosion potential index effects downstream sediment-transport rates causing higher transport.

Readers should be cautioned that the relation depicted in Figure 6-8 should not be used for predictive purposes. Still, the basinwide map of the upland erosion-potential index is useful as a general guide to help identify areas that can produce significant quantities of suspended sediment to Lake Tahoe streams.

6.3.4 Limitations of Analysis

A potential problem with one of the underlying assumptions of the analysis in relating the upland-erosion potential index with gaged sediment-transport rates is that upland sources will make up an unknown proportion of downstream sediment loads with the remainder emanating from channel sources. Thus, watersheds with high channel-erosion rates relative to upland contributions may not regress well with an upland-erosion index even if the index is accurately defining upland-erosion potential. Appropriately representing landuse/landcover over the time period of sampling at each downstream gaging station poses additional uncertainty because of land surface changes over the period, particularly in the northern quadrant of the basin. Finally,

because the mean- annual precipitation layer had the coarsest resolution, 20 by 20 m, the final raster layer had that resolution.

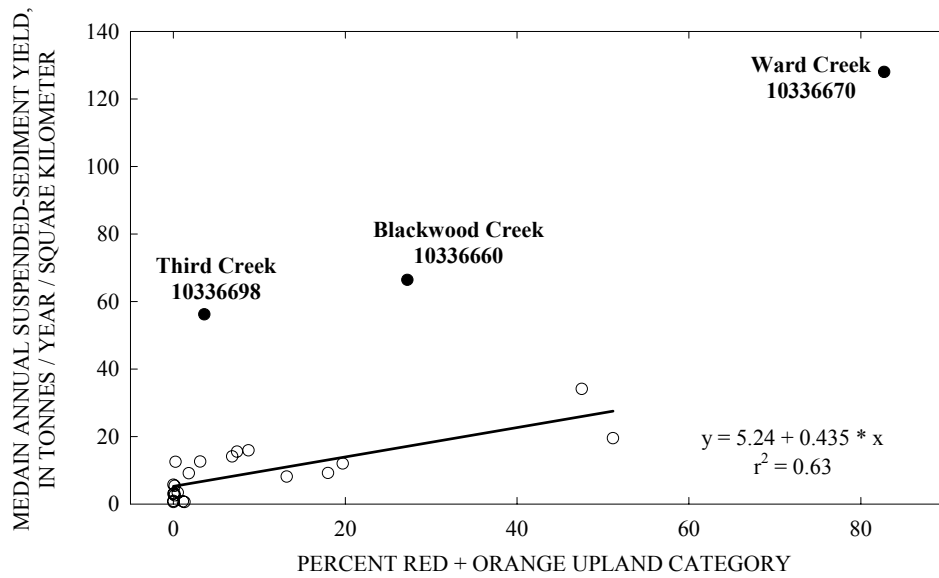


Figure 6-8. Relation between high upland-erosion potential and median, annual suspended-sediment yield.